What can decadal variability tell us about climate feedbacks and sensitivity?

Robert Colman and Scott B. Power

Australian Bureau of Meteorology,

Melbourne, Australia

January, 2018

Submitted to Climate Dynamics

Key Points:

- Strong positive radiative feedbacks operate at decadal timescales in climate models
- These feedbacks are correlated with the range of decadal temperature variability, particularly in the tropics
- Radiative feedbacks operating at decadal timescales are of the same magnitude as climate change feedbacks, and there is evidence for common physical processes on decadal and climate change timescales.
- There is evidence of a link between the magnitude of decadal variability and the model response to anthropogenic forcing in the latest set of models (CMIP5) although not in an earlier generation (CMIP3)

Address for correspondence:

Robert Colman,

Australian Bureau of Meteorology,

GPO Box 1289,

Melbourne, Victoria, 3001,

Australia

(robert.colman@bom.gov.au)

Abstract

Radiative feedbacks are known to determine climate sensitivity. Global top–of-atmosphere radiation correlations with surface temperature performed here show that decadal variability in surface temperature is also reinforced by strong positive feedbacks in models, both in the long wave (LW) and short wave (SW), offsetting much of the Planck radiative damping. Net top-of-atmosphere feedback is correlated with the magnitude of decadal temperature variability, particularly in the tropics. This indicates decadal-timescale radiative reinforcement of surface temperature variability. Assuming a simple global ocean mixed layer response, the reinforcement is found to be of a magnitude comparable to that required for typical decadal global scale anomalies. The magnitude of decadal variability in the tropics is uncorrelated with LW feedbacks, but it *is* correlated with total SW feedbacks, which are, in turn, correlated with tropical SW cloud feedback. Globally, water vapour/lapse rate, surface albedo and cloud feedbacks on decadal timescales are, on average, as strong as those operating under climate change. Together these results suggest that some of the physical processes responsible for setting the magnitude of global temperature change in the 21st century and climate sensitivity also help set the magnitude of the natural decadal variability. Furthermore, a statistically significant correlation exists between climate sensitivity and decadal variability in the tropics across CMIP5 models, although this is not apparent in the earlier generation of CMIP3 models. Thus although the link to sensitivity is not conclusive, this opens up potential paths to improve our understanding of climate feedbacks, climate sensitivity and decadal climate variability, and has the potential to reduce the associated uncertainty.

1. Introduction

While further human-forced global average warming appears inevitable (IPCC, 2013; Peters *et al*., 2013), the magnitude of projected late 21st century warming (ΔT_{Global} say) for a given scenario of future greenhouse gas emissions is uncertain (Meehl *et al*., 2007a; Collins *et al*., 2013). Despite major efforts to understand and reduce this uncertainty (Boucher *et al*., 2013; Collins *et al*., 2013), it remains large. This complicates decisions relating to climate change adaptation and mitigation, and adds hundreds of billions of dollars to the associated cost (Hope, 2015).

Future climate will also depend on natural decadal climate variability (DCV; Hawkins and Sutton, 2009, 2011; Kirtman *et al*., 2013; Power *et al*. 2006; Deser *et al*., 2012) -- and includes processes such as the Interdecadal Pacific Oscillation (Power *et al*. 1999; 2006; Folland *et al*. 1999; Kosaka and Xie, 2013). Despite the importance of this *internally-driven* DCV to climate and life on earth, relatively little is known about the physical processes underpinning it and the factors that determine its magnitude (Liu *et al*., 2012). A key feature of coupled model DCV is that the range in models is enormous. The standard deviation (SD) of global decadal variability (SD_{G_10y}) differs by a factor of more than four across Coupled Model Intercomparison Project phase 5 (CMIP5, Taylor *et al*., 2012) models – see below. What causes this range?

Differences in the El Niño-Southern Oscillation (ENSO) of course will play a role in decadal variability. Middlemas and Clement (2016) found around half the variance in the frequency of significant warming/cooling decades per century across CMIP5 models could be explained by the magnitude of decadal variations in their Nino3 sea

surface temperatures (SST). Importantly ENSO variability is itself associated with strong radiative feedbacks, both regionally (Bellenger *et al*., 2014; Li *et al*., 2015) and globally (Colman and Power, 2010; Colman and Hanson, 2016), suggesting it has the potential for a significant role in stochastic radiative forcing and decadal radiative feedback.

Although coupled ocean/atmosphere processes such as ENSO likely play a role in determining the magnitude of DCV, they are unlikely to be the whole story. It is notable that ocean models with only mixed layer physics can also show strong variability (Middlemas and Clement, 2016; Xie *et al*., 2016). Thus, although fully coupled models, as expected, do show larger variances across most timescales in both radiation and global temperature (Xie *et al*., 2016), the differences are relatively small at decadal and longer timescales. For example, there is only around 5% difference in the decadal SD of global temperature in mixed layer/fully coupled pair of models considered by Middlemas and Clement (2016). Consistent with this, a review by Liu (2012) concludes that processes involving ocean/atmosphere dynamical feedbacks play only a relatively minor role globally, although they may be important regionally (*e.g.* in the North Atlantic (Chen and Tung, 2014)). What other processes may be critical?

Following Roe (2009), *radiative feedbacks* may play a significant role in determining decadal variability of surface temperature. Xie *et al*. (2016) infer that short wave (SW) stochastic radiative forcing plays a potentially important role in DCV as they find it typically leads temperature by around one year. They find, however, that the correlation of *total* global averaged radiation with global surface temperature on decadal timescales is relatively weak – peaking at around -0.4 at a lag of around 2 years,

due to strongly offsetting long wave (LW) and SW responses. They deduce a net radiative feedback under variability that peaks at only around half the magnitude of the climate change feedback (-0.5$W/m^2/K$ versus ~ -1 $W/m^2/K$), arguing that differences in temperature and radiation patterns drive a different feedback response to that of climate change (see also Zhou *et al*., 2015).

The Xie *et al.* (2016) analysis does not clarify the reasons underlying the very large range in variability in models, however. Nor does it preclude an important role for radiative feedback in amplifying DCV, given such feedbacks oppose what would otherwise have been a strongly damping Planck[1] cooling term, analogous to the case under climate change (Bony *et al*., 2006; Roe, 2009). Indeed the weaker net negative feedback noted by Xie *et al*. (2016) indicate there are *as strong or stronger* positive feedbacks than under climate change – as noted previously by Colman and Hanson (2013). Furthermore the small total feedbacks identified by Xie *et al*. (2016) are the net result of very strong, but offsetting LW (R=-0.8) and SW (R=+0.7) correlations, confirming that strong radiative feedback processes are indeed operating in these models. Consistent with this view, a coupled model run with suppressed water vapour feedback, was found to have significantly lower *interannual* variability (Hall and Manabe, 1999).

[1] The Planck cooling refers to the hypothetical TOA LW radiative cooling that would take place for the climate system under a given surface warming if the atmosphere warmed uniformly with height at the same rate the surface temperature change (*i.e*. no lapse rate changes), and there were no changes to other radiatively sensitive parameters in the atmosphere/surface, such as to water vapour, clouds or surface albedo. The Planck cooling is not strictly a climate 'feedback' but instead represents the radiative damping of the climate system that would occur *in the absence of feedbacks* (Bony *et al*., 2006). Here it is listed in tables as a 'feedback' for simplicity of presentation.

Considering the radiative contributions to decadal-long warming trends in CMIP5 models, Brown *et al*. (2014) concluded that typically around half the global average warming may be attributable to the net top of atmosphere radiative feedback (with the SW dominating the response) – although with large variation between decades and an uncertain role for LW feedback. The remaining global warming was associated with non radiative-feedback related processes, such as redistribution of heat within the climate system (Brown *et al*., 2014)

The preceding discussion indicates that significant uncertainties remain in the role of radiative feedback (including the relative roles of LW/SW) in the magnitude and inter-model range of DCV, both globally and in the tropics. Understanding the causes of this large range is not simply of importance for evaluating and improving models – but also for understanding recent climate trends and the role of radiative reinforcement, and how 'typical' this may be (*e.g*. Brown *et al*., 2014). Recent findings (Andrews *et al.*, 2015; Zhou *et al*., 2016; Gregory and Andrews, 2016) suggest that large scale cloud redistributions, in the recent period have been responsible for global radiative responses which have suppressed warming, inconsistent with long term climate change feedbacks, or even typical decadal feedbacks (Brown *et al*., 2014). Since tropical variability has been identified as an important driver of global-scale temperature variability (Kosaka and Xie 2013; Dai *et al*. 2015; Meehl *et al.* 2012), a particular focus will be on tropical decadal variability, and the associated radiative feedbacks. If radiative feedbacks play a key role in amplifying decadal temperature variability then there arises the important question of possible links between the magnitude of DCV and climate change.

This paper addresses the following questions:

- How large is the spread in DCV in models, globally and in the tropics/extra-tropics? How large is the influence of ENSO variability on this range?
- How strong are the LW/SW and net decadal radiative feedbacks in models on decadal timescales? Are these correlated with the magnitude of the variability, and are they of a sufficient magnitude to 'explain' the range? Which feedbacks are most important globally and in the tropics/extra-tropics?
- How large are climate feedbacks under DCV compared with climate change?
- Are there links between the magnitude of DCV, either globally or in the tropics, with either temperature change projected over the next century or with climate sensitivity?

The paper is laid out as follows: The methodologies for calculation of variability and feedback, and the models used are described in Section 2. Section 3 contains results and discussion, with conclusions in Section 4.

2. Analysis of variability and radiative feedbacks

Up to 41 models from the Coupled Model Intercomparison Project Phase 5 (CMIP5) (Taylor *et al*., 2012) archive were used for the calculation of variability and feedbacks from pre-industrial runs. The full list used is given in supplementary material Table S1. 200 years of data were used for all models except for MIROC4h (100 years available). Not all models provided the fields needed for the calculation of all top of atmosphere (TOA) radiative feedbacks. Model data was first re-gridded to a common 2.5° latitude/ longitude grid; global/tropical/extra-tropical annual means calculated were then detrended by removal of a linear fit, to eliminate any drift. For most models this had

170 little impact on calculated variability. Decadal SDs were calculated following
171 application of a 10 year running mean. Eighteen models from the Coupled Model
172 Intercomparison Project Phase 3 (Meehl *et al*., 2007b) were also used. These are listed
173 in Table S2 of the supplementary material. Equilibrium climate sensitivity (ECS)
174 values were obtained from Randall *et al*. (2007) and Flato *et al*. (2013) for CMIP3 and
175 CMIP5 respectively.
176
177 Decadal (or interannual) LW/SW/Net radiative feedbacks were calculated as follows.
178 For the interannual case, global annual means were calculated for surface temperature
179 and for TOA LW, SW and net radiation (*e.g*. see Forster and Gregory, 2006). The (200)
180 radiation values were then regressed against the corresponding surface temperatures,
181 to give the global feedback. For tropical feedback, the calculation was repeated, but
182 with averages for both TOA radiation and surface temperatures calculated over the
183 tropics only. Decadal feedbacks were calculated using an identical approach, following
184 the application of a 10-year running mean to the radiation and temperature fields. Error
185 bars shown throughout were determined from the 80% confidence interval from
186 standard regression. More sophisticated fitting can be applied using a Bayesian
187 approach which samples the uncertainty range in the data point. This approach has
188 been found to provide similar confidence spread for these feedbacks (Colman and
189 Hanson, 2013). We show 80% rather than, say, 95% confidence range in these plots,
190 as it is illustrative of the uncertainty in calculation for the feedbacks and how that
191 varies/differs between models and feedbacks, but avoids the visual clutter of showing
192 larger error bars.
193

Individual process feedbacks (Table 2) were calculated using "radiative kernels" (Soden *et al*., 2008; Shell *et al*., 2008). The kernels used here were derived from the BMRC/CAWCR model (see Soden *et al*., 2008) and vary as a function of month, latitude, and (apart from surface albedo) atmospheric level. For the preindustrial runs, relevant fields were first averaged into decadal monthly means, then the radiative kernel applied to pairs of corresponding months between adjacent decades. Decadal annual means were then calculated, and global or tropical averages regressed against corresponding average temperature changes. Details of the methodology are described in Colman and Hanson (2013). For the calculation of climate change feedbacks, kernels were applied to pairs of months selected from decades beginning 2010 and 2090. After calculation of annual means, feedbacks were then calculated by normalising radiation change by global mean surface air temperature change.

'Scaled' decadal feedbacks (see Table 2 and associated discussion) were calculated following Armour *et al*. (2013) and Colman and Hanson (2016). The assumption here is that feedbacks are (to first order) invariant for a given geographic location – *i.e*. the same locally for both climate change and DCV. To calculate the implied decadal global or tropical feedback, local feedbacks obtained from kernel calculations under RCP8.5 were 'scaled' by the relative surface temperature variations that occur under DCV. Details on the approach are provided in Colman and Hanson (2016), and it is discussed further below. An important caveat is that some processes will not be expected to be only locally temperature dependent. For example Zhou *et al.* (2016) argue that East Pacific tropical cloud changes are affected by changes in West Pacific temperatures through changes in free tropospheric temperatures affecting inversion strength.

3. Results and discussion

Magnitude and pattern of decadal variability in models.

Figure 1 shows the SD of decadal global mean variability in surface air temperature in the CMIP5 models, ordered from lowest to highest. Values of SD range from 0.023 to 0.13 K. The range from the earlier CMIP3 models (Meehl *et al*., 2007b) was comparable: from 0.021 to 0.11 K (not shown). The processes resulting in this range remain unclear (Liu *et al*., 2012). For comparison, an observational estimate from Middlemas and Clement (2016) of DCV, obtained by removing estimates of forced changes to the GISTEMP data set (Hansen *et al*., 2010), is around 0.078K, *i.e.* towards the top of the model range (Fig. 1), therefore most models underestimate DCV (see also discussion in Laepple and Huybers, 2014; Fredrisken and Rypdal, 2016).

What does DCV look like spatially in the models and how does it compare to the patterns of climate change? Figure 2a shows the multi-model mean (MMM) of the change in local surface air temperature (for 2081-2100 relative to 1986-2005) under the RCP8.5 emissions scenario (van Vuuren *et al*., 2011). Figure 2b shows point-by-point regression of temperature against tropical mean temperature from the pre-industrial experiments (after application of a 10 year running mean) – *i.e*. the MMM DCV pattern *relative to tropical mean temperature change* (30° N to 30°S). Stippling indicates >70% of models agree on the sign of the change, which indicates statistical significance at the 95% level under the assumption of model independence (see supplementary material). Figure 2b shows a surprisingly high degree of coherence in internally generated DCV in T with variability in T averaged over the tropics. In the vast majority of locations, the models tend to warm when the tropics are warm, with

out-of-phase temperature variations restricted to a relatively small region in the North Pacific. The spatial correlation coefficient between the two plots is 0.24. Figure 2b is overall consistent in pattern with findings elsewhere from regression of local temperature against decadal global temperature, or from clustering of warming/cooling decades, suggesting that models reproduce IPO-like SST patterns under unforced DCV (Middlemas and Clement, 2016; Brown *et al*., 2015; Power *et al.*, 2016).

Decadal variability and tropical Pacific variability.

How important is ENSO variability for DCV? Figure 3 shows a plot of global and tropical variability against decadal NINO3.4 variability. Very little global variance can be explained by NINO3.4 (in agreement with the findings of Middlemas and Clement, 2016), but this increases to around 1/3 when only the tropics are considered. Other ENSO indices (NINO3, NINO4) give similar results to those of Fig. 3 (not shown). Note, however that all models produce NINO3.4 decadal SD below the estimated observational value from Middlemas and Clement (2016) of around 0.3K, so models may be underrepresenting the influence of ENSO on decadal variability. This view is consistent with Kociuba and Power (2015), which showed that models seemed to underestimate tropical DCV because of deficiencies in simulated ENSO characteristics. For *interannual* variability, the current analysis gives, as expected, much higher explained variances of 38% and 48% for model global and tropical variability magnitudes respectively, consistent with strong ENSO influence on interannual variability (*e.g.* Pan and Oort, 1983), but with decadal variations being less strongly associated with dynamical ocean/atmosphere feedback processes (Liu *et al*., 2012).

Decadal radiative feedbacks in models.

Which global and tropical mean TOA radiative feedbacks are associated with decadal variability? Before examining individual feedbacks, the *total* LW, SW and net radiative feedbacks are considered. These were determined from calculating 20 ten-year averages for each model using their pre-industrial runs, then regressing net TOA radiative variations against global average surface air temperature (see supplementary Fig. S1 for an example). It is found (consistent with Xie *et al.*, 2016) that strong correlations occur for both LW and SW with global mean temperature, but that the correlations are weaker when net feedback is considered, due to the offsetting nature of the LW/SW (*e.g.* supplementary Fig. S1).

The value of multi-model mean DCV-related global, tropical and extra-tropical LW, SW and Net feedbacks are given in Table 1. The inter-model SD is shown in brackets. Table 1 also shows the decadal LW feedback with the Planck term removed.

It is immediately apparent from Table 1 that setting aside the Planck cooling (see below), decadal feedbacks are strong and positive in both LW and SW, and make a close-to-equal contribution to positive feedback globally. Including the Planck cooling results in a 'total response' MMM radiative feedback of only -0.24 $W/m^2/K$, close to radiative neutrality, and with significantly less radiative damping than for forced climate change (Bony *et al*., 2006; Flato *et al*., 2013). Interestingly, the MMM extra-tropical LW feedback is less radiatively damping than tropical, despite the low latitude maximum of the dominant water vapour feedback (Colman and Hanson, 2016). Because of this the extra-tropics play a larger role than the tropics in setting the overall strength of the global feedback. This is consistent with Brown *et al*. (2015) (their Fig.

5) that the extra-tropics are important for explaining spread in radiative contributions to decadal warming/cooling trends.

Interannual feedbacks (shown in Table 1) tell a similar story, *i.e.* there are positive LW and SW feedbacks in both the tropics and extra-tropics. On interannual timescales, however, total radiative feedback is more damping than for DCV (by around 0.5 $W/m^2/K$), suggesting radiative feedbacks play a lesser role in amplifying variability at interannual compared with decadal timescales (see also Forster, 2016). Furthermore, ocean heat capacity is large, so the radiative heating would not change the climate system temperature much on interannual timescales. This is noted here but will not be further quantified in this paper.

How do decadal radiative feedbacks relate to the magnitude of model variability? Global (tropical) DCV is plotted against total global (tropical) TOA radiative feedback across the models in Fig. 4. Error bars show 80% confidence limits from standard regression of the radiative feedback magnitude (discussed in Section 2 above) or from the confidence limits in estimating decadal temperature SD from the 200-year pre-industrial experiments (*e.g.* Sheskin, 2016). A modest positive correlation (R=0.37) is apparent for global values, stronger (R=0.49) for the tropics-only case (*i.e.* for tropical DCV regressed against tropical radiation). Both regressions are statistically significant at the 95% level. This implies that models with stronger DCV, and particularly tropical variability, tend to have stronger positive (reinforcing) net TOA radiative feedback. By contrast, the equivalent regressions for interannual variability (not shown) are not statistically significant.

Note that two models have net positive feedback at decadal timescales in Fig. 4, raising the issue of their stability under variability. There are two important aspects here. Firstly, when considered at the 95% level only one model (MIROC-ESM) remains statistically greater than zero (not shown) – so further study is needed to confirm that its feedback is indeed positive. Secondly, even if at decadal timescales a model has no net radiative damping (or a small positive radiative feedback) this does not imply that this holds at all timescales – for example there are no positive feedback models at interannual timescales even at the 80% level (not shown). Physical damping factors that operate between different timescales – *e.g*. involving deep exchange of heat in the ocean, or involving negative feedbacks which result from differing surface temperature variability patterns, must act to stabilise the long term response. So even if the climate system were to gain energy at decadal timescales, it must lose energy to other timescales. Such interactions are likely complex, and investigation of them lies beyond the scope of this paper.

Comparing feedback processes under decadal variability and climate change.

To understand what sets the magnitude of the SW/LW feedbacks we must examine the contributions from differing processes. Individual (global) MMM decadal feedbacks for surface temperature (Planck), water vapour, lapse rate, surface albedo and clouds, along with their inter-model SD, are provided in Table 2. Also shown, for comparison, are global climate change feedbacks. The bottom two rows show the net feedback calculated by summing the individual feedback terms, and can be compared with the total feedbacks calculated by straight regression of TOA net SW/LW radiation. It can be seen that the numbers are close, although not exact. Uncertainty of kernel calculations (Soden *et al.,* 2008) will play some role in this difference, but differences

arise from the uncertainties inherent in the estimation of decadal feedbacks (especially clouds) from the (only) 200 year timeseries. Given the independent methods of the two calculations, however, the overall agreement bolsters confidence in the calculations of the individual feedback terms.

The source of the strong decadal feedbacks can be seen in Table 2. LW and SW water vapour feedbacks are, on average, comparable to those of climate change (LW component around 20% weaker). Together these provide about 60% of the total positive feedback. Decadal lapse rate feedback is close to neutral, compared to a negative climate change feedback of -0.74 $W/m^2/K$, and mean that the combined water vapour/lapse rate feedback contributes a similar fraction of overall positive feedback at decadal timescales as under forced climate change. For clouds, the MMM SW cloud feedbacks are comparable for DCV and climate change. The DCV LW cloud feedback is a little weaker than the corresponding climate change feedback (although still positive). Perhaps surprisingly, the surface albedo feedback is stronger in the decadal case. The inter-model spread of the decadal albedo feedback is very large, and models show an extremely large range in the coverage of sea ice in their pre-industrial climate (Hobbs *et al*., 2016), so at least part of the spread may arise from consequent differences in sea ice response. We hope to investigate this in a future study.

The reasons for these overall similarities in climate change/decadal feedback strength are not immediately clear, but the similarities in the temperature response to global or tropical temperature change under climate change and DCV (Fig. 2) may imply similar radiative feedback responses. Recent results (Armour *et al*., 2013) have found that treating feedbacks as 'locally unchanging' (that is, fixed in strength at particular

368 locations, with the global feedback strength then dependent on the contribution of local
369 feedbacks) can explain the evolution of global feedbacks in long climate change
370 experiments from changes in the global surface temperature pattern. Colman and
371 Hanson (2016) performed calculations for decadal feedbacks following this approach
372 based on 'local' feedbacks derived from RCP8.5 experiments. The MMM strength
373 (and intermodal variation) of feedbacks from the decadal Planck response, LW and SW
374 water vapour and surface albedo feedbacks (Table 2) are indeed recovered from the
375 scaling. LW cloud feedback is also reasonably reproduced, but lapse rate and SW
376 cloud feedbacks show significant differences. These results suggest that the patterns
377 of warming in Fig. 2 may be 'similar enough' for common processes to be operating
378 for most radiative feedbacks under both climate change and decadal variability
379 (Colman and Hanson, 2016).
380
381 Further evidence of the similarities in processes between feedbacks operating under
382 climate change and DCV come from: (i) common patterns of vertical contributions to
383 water vapour and lapse rate feedbacks (Colman and Power, 2010; Colman and Hanson;
384 2013); (ii) a water vapour feedback that is consistent with unchanged relative humidity
385 (Colman and Hanson, 2013); and (iii) an inverse relationship between lapse rate and
386 (LW) water vapour feedback (Colman and Hanson, 2013). Correlations have also
387 been found between the strength of interannual and climate change net cloud feedback
388 across models (Zhou *et al*., 2015). Finally, global variability on interannual timescales
389 has also been shown to be reduced when global radiative feedbacks are suppressed
390 (Hall and Manabe, 1999; Hall 2004), and ENSO-associated variability reduced when
391 cloud feedbacks are suppressed (Ying and Huang, 2016; Radel *et al*., 2016). Overall
392 then, there is evidence for strong positive radiative feedbacks operating in models as

well as similarities in the feedback strengths and structures between decadal (and interannual) variability and climate change.

But are inter-model decadal feedback differences enough to explain (or at least contribute substantially to) the range in DCV? Table 2 shows a MMM positive feedback of around +2.5 $W/m^2/K$, with a *range* of ~2 $W/m^2/K$ – see Fig. 4. This variation comes from the terms offsetting the Planck cooling; as the latter is tightly clustered around -2.95 $W/m^2/K$ with relatively small SD across models. Assuming the simplest possible (zero dimensional) feedback reinforcement of temperature deviations (see supplementary material) under a global ΔT of 0.05K (MMM SD of DCV – Fig. 1), a positive feedback of 2 $W/m^2/K$ is sufficient to provide reinforcing warming of ~0.075K to a global mix-layer of 100m depth on decadal timescales. There will be some sensitivity of this warming figure to assumptions about factors like the mixed layer depth, but the figure chosen here is consistent with those chosen elsewhere in decade timescale changes under global warming (Geoffroy *et al*., 2012; Brown *et al*., 2014). This temperature change is the same order as the SD of temperature variation itself and provides *prima facie* evidence that positive feedbacks in the models can induce temperature excursions of the appropriate magnitude for DCV (consistent with the results of Brown *et al*., 2014).

We would expect several factors to contribute to the magnitude of variability that are not considered here. Theoretical arguments (*e.g.* Roe, 2009) indicate variability should increase with the magnitude of stochastic forcing (such as from ENSO variability, Trenberth *et al.*, 2002 or from short timescale cloud variations, Trenberth *et al*., 2014), and decrease with ocean thermal inertia and radiative damping. For example, CMIP5

models show a broad range of effective ocean depth, on climate change timescales at least (Geoffroy *et al.*, 2012), and are likely to do so on interannual and decadal timescales. However in the present study we only consider the influence of the radiative damping term. A consideration of the roles of oceanic mixing and magnitude of stochastic forcing in determining model interannual/decadal variability is to be the subject of a follow up study.

It is known that clouds and SW cloud feedbacks in particular are responsible for much of the range in total feedback under climate change (Bony and Dufresne, 2005; Boucher *et al*., 2013). What individual feedbacks are most important for the range in decadal net feedback? The separate variation of tropical SW and LW total decadal feedback against tropical DCV (Fig 5.) reveals no relationship between variability and LW feedback, but a strong (and statistically significant at the 95% level) positive correlation in the SW (R=0.58). The situation is qualitatively similar at global scales, although the SW correlation with variability is weaker (R=0.33) and not statistically significant in this case (not shown). Therefore, although LW feedback plays a roughly equal role with the SW in the overall amplification of the variability of DCV, the SW is primarily responsible for the differing responses in net feedback between models.

The total SW tropical feedbacks is in turn correlated with strength of the SW cloud feedbacks in models (R=0.56, Fig. 6). This provides evidence that differences in cloud responses on decadal timescales may provide an important mechanism for net tropical variability, and echoes the role that SW cloud responses – particularly in the tropics – play in determining climate change sensitivity (Bony and Dufresne, 2005, Andrews *et al.*, 2012; Webb *et al.*, 2015; Zelinka *et al.*, 2013). A statistically significant (at the

95% level) offsetting relationship is also apparent between total LW and SW feedbacks both for the tropics and globally: Fig. 7 (R=-0.41, and R=-0.56, respectively). This means that the net feedback range is smaller than it would otherwise be, since stronger (positive) feedback in the SW implies weaker (negative) feedback in the LW. The correlations found here are suggestive of an important role of radiative feedbacks and in particular of tropical clouds in decadal timescale tropical variability, but do not conclusively establish it. Furthermore, there is no significant negative correlation between LW/SW cloud feedbacks themselves across models (not shown), so the causes of the inverse LW/SW radiative feedback relationship remain unclear and require further investigation.

Is there a link between decadal temperature variability and climate change?

How do these results relate to climate change? Given the widespread coherence of DCV in surface temperature over the globe with tropical DCV in surface temperature (Fig. 2b), and the apparent role of radiative feedbacks in tropical DCV discussed above, we hypothesize that model-to-model differences in the magnitude of internal DCV might be related to model-to-model differences in the magnitude of ΔT_{Global}. This is confirmed for the CMIP5 models in Fig. 8a, which shows that ΔT_{Global} and the SD of DCV in $T_{Tropics}$ (SD_{T_10y}) are linearly correlated, with a correlation coefficient of 0.60 (Table 3), which is statistically significant at the 95% confidence level. The correlation coefficient increases to 0.73 if attention is restricted to $\Delta T_{Tropics}$, the projected change in tropical temperature (Fig. 8b).

The sensitivity of climate change to imposed anthropogenic forcing can also be measured using the Equilibrium Climate Sensitivity (ECS) and the Transient Climate

Response (TCR) indices (Collins *et al*., 2013). The ECS is plotted against ΔT_{Global} in Fig. 8c, showing a very high correlation coefficient. TCR is, as expected, strongly correlated with ECS, although TCR is less closely correlated with ΔT_{Global} than is ECS (not shown). These findings are consistent with the results of Gregory *et al*. (2015) and Grose *et al*. (2016). The relationships between SD_{T_10y} and all of ΔT_{Global}, ECS and the TCR are consistent in the sense that the degree of warming and the sensitivity tends to be larger in models with larger values of SD_{T_10y}.

Correlating SD_{T_10y} against ECS in CMIP5 models (Fig. 9a) reveals a statistically significant correlation, with SD_{T_10y} explaining nearly half the variance in ECS. A statistically significant correlation also holds between global SD_{10y} and ECS, but it is weaker (R=0.42) (not shown). So the CMIP5 models suggest there is indeed a link between SD_{T_10y} and climate sensitivity.

As a further test we examined the same issue in CMIP3 models. Despite the relationships found in CMIP5, no such relationships (*e.g.* between ECS and SD_{T_10y}) are found for the earlier set of CMIP3 models (Fig. 9b). This does not automatically rule out a relationship between DCV and ECS: CMIP5 models show improvement, including in climate variability, over CMIP3 models (Flato *et al*., 2013). For example biases in the tropical Pacific mean state are reduced and ENSO related variability better represented (Flato *et al*., 2013; Bellenger *et al*., 2014). However there is 'no quantum leap in ENSO performance' (Bellenger *et al*., 2014), nor is there an overall reduction in the range of DCV in CMIP5 compared with CMIP3 (see above). Therefore it remains unclear whether the links between DCV and ECS/ΔT_{Global} revealed in CMIP5 models are robust. It will be of interest to explore possible decadal variability/ECS

correlations within the upcoming CMIP6 group of models, particularly if, as expected, ENSO-related variability is further improved and tropical biases further reduced. The present results suggest, at the very least, that further research is warranted in this area.

4. Conclusions

Ongoing uncertainty in climate change projections arise from the range of model ECS, and this range has not narrowed in the last two decades (*Flato et al.*, 2013). At the same time, DCV varies by at least a factor of 4 across CMIP5 models (and varied by a similar range in CMIP3). Understanding the causes of both of these ranges are critical tasks in climate change science.

The present results provide evidence that global scale radiative feedbacks are playing an important role in the magnitude of global and tropical DCV in CMIP5 models. Both SW and LW feedbacks are positive globally, and LW feedback is as important as the SW in setting the magnitude of the overall feedback. The *differences* between total feedback globally in models are primarily due to the SW component. The strength of this feedback is, in turn, correlated with SW cloud feedback, and this is particularly strong in the tropics. ENSO related variability certainly plays a role in the spread, with results here suggesting around 1/3 of the *tropical* variance is related to central Pacific DCV – although very little *global* spread is explained. This is consistent with findings elsewhere that deficiencies in representation of ENSO have a substantial impact on tropical temperature DCV (Kociuba and Power, 2014)

SW/LW feedbacks also tend to offset one another both in the tropics and globally. This suggests related but opposing SW/LW processes, particularly from clouds. However, puzzlingly, regressions across models between the strength of the SW/LW cloud feedbacks do not show significant anti-correlations. It should be noted that clouds show high stochastic variability, and that long periods may be required to accurately estimate cloud feedbacks (Colman and Hanson, 2013). Further research is needed to clarify the role of clouds in decadal feedback spread, and in the offsetting SW/LW components.

Most radiative feedback components show comparable overall strength in the MMM on decadal and climate change timescales (except most noticeably for global lapse rate). Furthermore the global MMM decadal feedback strength can, for all components except lapse rate and SW cloud, be recovered simply by scaling the climate change feedback by the relative temperature warming found in DCV per degree of global temperature change. A simple zero-dimensional calculation of decadal heating resulting from the positive feedback shows the magnitude of positive feedbacks in models can induce temperature reinforcement of the order of 0.075K in a 100m deep ocean on decadal timescales, the same magnitude of the decadal temperature deviations themselves.

Taken together this evidence suggests that radiative feedbacks operating on decadal timescales may shed critical light on the processes controlling the magnitude of projected changes. It is suggestive that for the CMIP5 models a correlation exists between ECS and DCV, and this correlation is particularly strong for tropical variability, although earlier CMIP3 models, does not reproduce this relationship. The

543 CMIP3 results lower the confidence in the existence of a link between the magnitude
544 of DCV and climate sensitivity, but does not preclude the possibility, especially since
545 CMIP5 models are superior to CMIP3 models in many respects (Flato *et al.*, 2013). It
546 will be important to retest our key hypothesis with the next generation of models.
547 Further research on decadal radiative feedbacks, their role in variability, and their
548 relationship with climate change feedbacks is needed.
549

Acknowledgements

We thank Greg Kociuba for analysis and generating some of the figures and Guomin Wang, Lawson Hanson and François Delage with assistance with aspects of the analysis, and Josephine Brown and Christine Chung for helpful comments on the manuscript. This work was supported by the Australian National Environmental Science Programme. We acknowledge the World Climate Research Programme's Working Group on Coupled Modelling, which is responsible for CMIP, and we thank the climate modelling groups for producing and making available their model output. For CMIP the U.S. Department of Energy's Program for Climate Model Diagnosis and Intercomparison provides coordinating support and led development of software infrastructure in partnership with the Global Organization for Earth System Science Portals.

References

Andrews, T., J.M. Gregory and M.J. Webb (2015), The dependence of radiative forcing and feedback on evolving patterns of surface temperature change in climate models. J. Clim. 28, 1630-1648

Andrews T., J.M. Gregory, M.J. Webb and K.E. Taylor (2012): Forcing, feedbacks and climate sensitivity in CMIP5 coupled atmosphere-ocean climate models. Geophys. Res. Lett. 39:L09,712 doi:10.1029/2012GL051607

Armour, K.C., C.M. Bitz and G.H. Roe (2013): Time-Varying Climate Sensitivity from Regional Feedbacks. J. Clim., 26, 4518-4534, doi: 10.1175/JCLI-D-12-00544.1.

Bellenger, H., E. Guilyardi, J. Leloup, M. Lengaigne, and J. Vialard (2014): ENSO representation in climate models: From CMIP3 to CMIP5. Climate Dyn., 42, 1999–2018, doi:10.1007/s00382-013-1783-z.

Bony, S., R.A. Colman, V. Kattsov, R.P. Allan, C.S. Bretherton, J.-L. Dufresne, A. Hall, S. Hallegatte, M.M. Holland, W. Ingram, D.A. Randall, B.J. Soden, G. Tselioudis and M.J. Webb (2006): How well do we understand and evaluate climate change feedback processes? J. Clim., 19, 3445-3482.

Bony, S. and J.-L. Dufresne (2005), Marine boundary layer clouds at the heart of tropical cloud feedback uncertainties in climate models, Geophys. Res. Lett., 32, L20806, doi:10.1029/2005GL023851.

Boucher, O., D. Randall, P. Artaxo, C. Bretherton, G. Feingold, P. Forster, V.-M. Kerminen, Y. Kondo, H. Liao, U. Lohmann, P. Rasch, S.K. Satheesh, S. Sherwood, B. Stevens and X.Y. Zhang (2013): Clouds and Aerosols. In: Climate Change 2013: The Physical Science Basis. Contribution of Working Group I to the Fifth Assessment Report of the Intergovernmental Panel on Climate Change [Stocker, T.F., D. Qin, G.-K. Plattner, M. Tignor, S.K. Allen, J. Boschung, A. Nauels, Y. Xia, V. Bex and P.M. Midgley (eds.)]. Cambridge University Press, Cambridge, United Kingdom and New York, NY, USA.

Brown, P.T., W. Li, L. Li, and Y. Ming (2014), Top-of-atmosphere radiative contribution to unforced decadal global temperature variability in climate models, Geophys. Res. Lett., 5175–5183, doi:10.1002/2014GL060625.

Brown, P.T., W. Li, and S.-P. Xie (2015), Regions of significant influence on unforced global mean surface air temperature variability in climate models, J. Geophys. Res. Atmos., 120, 480–494, doi:10.1002/2014JD022576.

Chen, X., and K.-K. Tung (2014): Varying planetary heat sink led to global-warming slowdown and

592 acceleration. Science, 345, 897–903, doi:10.1126/science.1254937.
593 Collins, M., R. Knutti, J. Arblaster, J.-L. Dufresne, T. Fichefet, P. Friedlingstein, X. Gao, W.J. Gutowski,
594 T. Johns, G. Krinner, M. Shongwe, C. Tebaldi, A.J. Weaver and M. Wehner (2013): Long-term
595 Climate Change: Projections, Commitments and Irreversibility. In: Climate Change 2013: The
596 Physical Science Basis. Contribution of Working Group I to the Fifth Assessment Report of the
597 Intergovernmental Panel on Climate Change [Stocker, T.F., D. Qin, G.-K. Plattner, M. Tignor,
598 S.K. Allen, J. Boschung, A. Nauels, Y. Xia, V. Bex and P.M. Midgley (eds.)]. Cambridge
599 University Press, Cambridge, United Kingdom and New York, NY, USA.
600 Colman, R.A. and S.B. Power (2010): Atmospheric feedbacks associated with transient climate change
601 and climate variability. Clim. Dyn., 34, 919-934, doi: 10.1007/s00382-009-0541
602 Colman, R.A. and L.I. Hanson (2013): On atmospheric radiative feedbacks associated with climate
603 variability and change. Clim. Dyn., 40, 475-492, doi 10.1007/s00382-012-1391-3.
604 Colman, R.A. and L.I. Hanson (2016): On the relative strength of radiative feedbacks under climate
605 variability and change, Clim. Dyn., doi:10.1007/s00382-016-3441-8.
606 Dai, A., J.C. Fyfe, S.-P. Xie, X. Sai, (2015): Decadal modulation of global surface temperature by
607 internal climate variability. Nature Climate Change, 5, 555–559, doi:10.1038/nclimate2605.
608 Deser, C., A. Phillips, V. Bourdette, H. Teng (2012): Uncertainty in climate change projections: the role
609 of internal Variability, Clim Dyn (2012) 38:527–546, DOI 10.1007/s00382-010-0977-x.
610 Flato, G., J. Marotzke, B. Abiodun, P. Braconnot, S.C. Chou, W. Collins, P. Cox, F. Driouech, S. Emori,
611 V. Eyring, C. Forest, P. Gleckler, E. Guilyardi, C. Jakob, V. Kattsov, C. Reason and M.
612 Rummukainen (2013): Evaluation of Climate Models. In: Climate Change 2013: The Physical
613 Science Basis. Contribution of Working Group I to the Fifth Assessment Report of the
614 Intergovernmental Panel on Climate Change [Stocker, T.F., D. Qin, G.-K. Plattner, M. Tignor,
615 S.K. Allen, J. Boschung, A. Nauels, Y. Xia, V. Bex and P.M. Midgley (eds.)]. Cambridge
616 University Press, Cambridge, United Kingdom and New York, NY, USA.
617 Folland, C. K., D. E. Parker, A. Colman and R. Washington (1999): Large scale modes of ocean surface
618 temperature since the late nineteenth century. p. 73–102. In Beyond El Niño: Decadal and
619 Interdecadal Climate Variability, ed. by A. Navarra, Springer-Verlag, Berlin, 374 pp.
620 Forster, P.M.de F (2016): Inference of Climate Sensitivity from Analysis of Earth's Energy Budget.
621 Ann. Review of Earth and Planetary Sciences, 44, 85-106.

622 Forster, P.M.de F. and J.M. Gregory (2006): The Climate Sensitivity and Its Components Diagnosed
623 from Earth Radiation Budget Data. J. Clim., 19, 39-52.
624 Fredriksen, H-B. and K. Rypdal (2016): Spectral Characteristics of Instrumental and Climate Model
625 Surface Temperatures. J. Clim., 29, 1253-1268. doi: 10.1175/JCLI-D-15-0457.1
626 Geoffroy, O., D. Saint-Martin, D. J. L. Olivié, A. Voldoire, G. Bellon, and S. Tytéca (2012), Transient
627 Climate Response in a Two-Layer Energy-Balance Model. Part I: Analytical Solution and
628 Parameter Calibration Using CMIP5 AOGCM Experiments, J. Clim., 26, 1841-1857,
629 doi:10.1175/JCLI-D-12-00195.1.
630 Gregory, J.M. and Andrews, T. (2016), Variation in climate sensitivity and feedback parameters during
631 the historical period. Geophys. Res. Lett. 43, 3911-3920.
632 Gregory J.M., Andrews T., Good P. (2015), The inconstancy of the transient climate response parameter
633 under increasing CO2. Phil.Trans.R.Soc.A 373: 20140417.
634 Grose, M.R., R.A. Colman, J. Bhend and A.F Moise (2016): Limits to global and Australian temperature
635 change this century based on expert judgment of climate sensitivity, Clim. Dyn., doi:
636 10.1007/s00382-016-3269-2.
637 Hall, A. and S. Manabe (1999): The role of water vapour feedback in unperturbed climate variability
638 and global warming. J. Clim., 12, 2327–2346.
639 Hall A. (2004): The role of surface albedo feedback in climate. J. Clim., 17, 1550–1568. DOI:
640 10.1175/1520-0442(2004)017
641 Hansen, J., R. Ruedy, M. Sato, and K. Lo (2010): Global surface temperature change, Rev. Geophys.,
642 48, RG4004, doi:10.1029/2010RG000345.
643 Hawkins, E. and Sutton, R. (2009). The Potential to Narrow Uncertainty in Regional Climate
644 Predictions. Bulletin of the American Meteorological Society 90: 1095-1107.
645 Hawkins, E. and Sutton, R. (2011). The potential to narrow uncertainty in projections of regional
646 precipitation change. Clim. Dyn. 37: 407-418.
647 Hobbs W.R., R. Massom, S. Stammerjohn, P. Reid, G. Williams and W. Meier (2016), A review of
648 recent changes in Southern Ocean sea ice, their drivers and forcings, Global and Planetary
649 Change 14, 228–250
650 Hope C. (2015), The $10 trillion value of better information about the transient climate response.
651 Phil.Trans.R.Soc.A 373: 20140429. http://dx.doi.org/10.1098/rsta.2014.0429

IPCC (2013): Summary for Policymakers. In: Climate Change 2013: The Physical Science Basis. Contribution of Working Group I to the Fifth Assessment Report of the Intergovernmental Panel on Climate Change [Stocker, T.F., D. Qin, G.-K. Plattner, M. Tignor, S.K. Allen, J. Boschung, A. Nauels, Y. Xia, V. Bex and P.M. Midgley (eds.)]. Cambridge University Press, Cambridge, United Kingdom and New York, NY, USA.

Kirtman, B., S.B. Power, J.A. Adedoyin, G.J. Boer, R. Bojariu, I. Camilloni, F.J. Doblas-Reyes, A.M. Fiore, M. Kimoto, G.A. Meehl, M. Prather, A. Sarr, C. Schär, R. Sutton, G.J. van Oldenborgh, G. Vecchi and H.J. Wang (2013): Near-term Climate Change: Projections and Predictability. In: Climate Change 2013: The Physical Science Basis. Contribution of Working Group I to the Fifth Assessment Report of the Intergovernmental Panel on Climate Change [Stocker, T.F., D. Qin, G.-K. Plattner, M. Tignor, S.K. Allen, J. Boschung, A. Nauels, Y. Xia, V. Bex and P.M. Midgley (eds.)]. Cambridge University Press, Cambridge, United Kingdom and New York, NY, USA.

Kociuba, G. and S.B. Power (2015): Inability of CMIP5 Models to Simulate Recent Strengthening of the Walker Circulation: Implications for Projections. J. Clim., 28, 20-35. Doi: 10.1175/JCLI-D-13-00752.1.

Kosaka, Y., and S.-P. Xie, 2013: Recent global-warming hiatus tied to equatorial Pacific surface cooling. Nature, 501, 403-407, doi:10.1038/nature12534.

Laepple, T. and P. Huybers (2014): Ocean surface temperature variability: Large model-data differences at decadal and longer periods. PNAS, 111, 16682–16687, doi: 10.1073/pnas.141207711.

Li, L., B. Wang and G.J. Zhang (2015): The Role of Moist Processes in Shortwave Radiative Feedback during ENSO in the CMIP5 Models, J. Clim., 28: 9892–9908, DOI: http://dx.doi.org/10.1175/JCLI-D-15-0276.1

Liu, Z. (2012), Dynamics of interdecadal climate variability: A historical perspective. J. Clim. 25, 1963-1995. DOI: 10.1175/2011JCLI3980.1

Meehl, G. A., *et al*. (2007a) : Global climate projections. In *Climate Change 2007: The Physical Science Basis. Contribution of Working Group I to the 4th Assessment Report of the Intergovernmental Panel on Climate Change*, edited by S. Solomon *et al*., pp.747– 845, Cambridge Univ. Press, New York.

Meehl, G. A., C. Covey, K. E. Taylor, T. Delworth, R. J. Stouffer, M. Latif, B. McAvaney, and J. F. B. Mitchell, (2007b): The WCRP CMIP3 multimodel dataset: A new era in climate change research.

Bull. Amer.Meteor. Soc., 88, 1383–1394, doi:10.1175/BAMS-88-9-1383.

Meehl, G.A., A. Hu, J. M. Arblaster, J. Fasullo, and K.E. Trenberth (2012): Externally Forced and Internally Generated Decadal Climate Variability Associated with the Interdecadal Pacific Oscillation. J. Climate, 26, 7298-7310, DOI: http://dx.doi.org/10.1175/JCLI-D-12-00548.1.

Middlemas, E., and A. Clement, (2016): Spatial patterns and frequency of unforced decadal scale changes in global mean surface temperature in climate models. J. Clim.., 29, 6245-6257, doi:10.1175/JCLI-D-15-0609.1

Pan, Y. H., and A. H. Oort, (1983): Global climate variations connected with sea surface temperature anomalies in the eastern equatorial Pacific Ocean for the 1958–73 period. Mon. Wea. Rev., 111, 1244–1258, doi:10.1175/1520-0493(1983)111,1244: GCVCWS.2.0.CO;2.

Peters, G. P., R. M. Andrew, T. Boden, J. G. Canadell, P. Ciais, C. Le Quéré, G. Marland, M. R. Raupach, and C. Wilson (2013): The challenge to keep global warming below 2˚C. Nature Climate Change, **3**, 4-6

Power, S.B., T. Casey, C. Folland, A. Colman, and Mehta, V. (1999). Interdecadal modulation of the impact of ENSO on Australia. *Clim. Dyn*., **15**, 234– 319.

Power, S.B., F. Delage, G. Wang, I. Smith and G. Kociuba (2016). Apparent limitations in the ability of CMIP5 climate models to simulate recent multi‐decadal change in surface temperature: implications for global temperature projections. *Clim. Dyn*., doi:10.1007/s00382-016-3326-x

Power, S.B., M.H. Haylock, R. Colman, and X. Wang (2006): The predictability of interdecadal changes in ENSO activity and ENSO teleconnections. J. Clim., 19, 4755–4771 .

Rädel, G., T.Mauritsen, B. Stevens, D. Dommenget, D. Matei, K. Bellomo and A. Clement, (2016): Amplification of El Niño by cloud longwave coupling to atmospheric circulation, Nature Geoscience, 9,106–110, doi:10.1038/ngeo2630.

Randall, D.A. and co-authors (2007): Climate Models and Their Evaluation. In: Climate Change 2007: The Physical Science Basis. Contribution of Working Group I to the Fourth Assessment Report of the IPCC [Solomon, S., *et al*. (eds.)]. Cambridge University Press, Cambridge, United Kingdom and New York, NY, USA.

Roe, G. (2009). Feedbacks, timescales, and seeing red. Annual Review of Earth and Planetary Sciences 37, 93—115

Shell, K., J. Kiehl, and C. Shields (2008): Using the radiative kernel technique to calculate climate

feedbacks in NCAR's Community Atmospheric Model. J. Clim., 21, 2269–2282.

Sheskin, D.J. (2016): Handbook of Parametric and Nonparametric Statistical Procedures, IBSN:1439858012.

Soden, B.J., I.M. Held, R.A. Colman, K.M. Shell, J.T. Kiehl and C.A. Shields (2008): Quantifying Climate Feedbacks using Radiative Kernels. J. Clim., 21, 3504-3520, doi: 10.1175/2007JCLI2110.1

Taylor, K.E., R.J. Stouffer, and Meehl, G.A. (2012): An overview of the CMIP5 and the experimental design. *Bull. American Meteorol. Soc*., 485-498.

Trenberth, K.E., J.M. Caron, D.P. Stepaniak and S. Worley (2002): Evolution of El Niño–Southern Oscillation and global atmospheric surface temperatures. Journal of Geophysical Research: Atmospheres, 107, D8, 4065, doi: 10.1029/2000JD000298

Trenberth, K.E., J.T. Fasullo and M.A. Balmaseda (2014): Earth's energy imbalance. J. Climate 27, 3129-3144.

van Vuuren *et al.* (2011) The representative concentration pathways: an overview. *Climatic Change*, **109**, 5–31, doi:10.1007/s10584-011-0148-z

Webb, M., and Coauthors, (2015): The impact of parametrized convection on cloud feedback. Philos. Trans. Roy. Soc. London, A373, 20140414, doi:10.1098/rsta.2014.0414.

Xie, S.-P., Y. Kosaka, and Y. M. Okumura, (2016): Distinct energy budgets for anthropogenic and natural changes during global warming hiatus. Nat. Geosci., 9, 29–34, doi:10.1038/ngeo2581

Ying, J. and P. Huang, (2016): Cloud–Radiation Feedback as a Leading Source of Uncertainty in the Tropical Pacific SST Warming Pattern in CMIP5 Models. J. Clim., 29, 3867-3881, DOI: 10.1175/JCLI-D-15-0796.1

Zelinka, M. D., S. A. Klein, K. E. Taylor, T. Andrews, M. J. Webb, J. M. Gregory, and P. M. Forster (2013), Contributions of different cloud types to feedbacks and rapid adjustments in CMIP5, J. Clim., 26, 5007–5027.

Zhou, C., M.D. Zelinka, A.E. Dessler and S.A. Klein (2015): Relationship between cloud feedbacks in response to climate change and variability. Geophys. Res. Lett., 42,10,463–10,469, doi:10.1002/2015GL066698.

Zhou, C., M.D. Zelinka and S.A. Klein (2016): Impact of decadal cloud variations on the Earth's energy budget, Nature Geoscience, doi:10.1038/NGEO2828

743 **Tables**

744

745 **Table 1**: Global, tropical (30°N to 30°S) and extra-tropical (poleward of 30°) multi-
746 model mean LW, SW and net feedbacks under decadal and interannual variability.
747 Also shown is the LW with the Planck cooling term removed. Units are $W/m^2/K$.
748 Feedbacks are calculated by regressing area mean TOA radiation changes against
749 corresponding area mean temperature. Numbers in brackets represent 1 SD of model
750 spread.

751

		Global	Tropics	Extra-tropics
Decadal	LW	-1.52 (0.32)	-2.07 (0.72)	-0.90 (0.27)
	SW	1.28 (0.47)	1.58 (0.93)	0.88 (0.35)
	Total	-0.24 (0.40)	-0.48 (0.88)	-0.02 (0.21)
	LW (No Planck)	1.39 (0.28)	1.36 (0.62)	1.51 (0.39)
Interannual	LW	-1.57 (0.44)	-2.49 (0.80)	-0.89 (0.23)
	SW	0.81 (0.64)	1.56 (0.98)	0.71 (0.29)
	Total	-0.76 (0.62)	-0.93 (0.94)	-0.18 (0.31)

752

753 **Table 2**: Multi-model mean decadal and climate change global feedbacks. Units are
754 $W/m^2/K$. Feedbacks shown are surface temperature (Ts), LW/SW water vapour (q),
755 lapse rate (LR), surface albedo (a) and LW/SW cloud (C). Rightmost column shows
756 feedbacks derived by scaling local climate change feedback strength by the ratio of
757 decadal local temperature change per degree of global temperature rise to that from
758 climate change (Colman and Hanson, 2016). Bottom two rows show the sum of LW
759 and SW feedbacks for decadal and climate change feedbacks (for comparison with
760 results in Table 1).
761

Feedback	Decadal	Climate Change	Decadal derived from scaled climate change
Ts	-2.94 (0.13)	-3.07 (0.09)	-2.83 (0.21)
q (LW)	1.42 (0.49)	1.75 (0.19)	1.43 (0.38)
q (SW)	0.22 (0.05)	0.26 (0.04)	0.26 (0.06)
LR	0.0 (0.48)	-0.74 (0.23)	-0.53 (0.40)
a	0.78 (0.38)	0.42 (0.11)	0.70 (0.26)
C (SW)	0.20 (0.52)	0.19 (0.43)	-0.26 (0.41)
C (LW)	0.23 (0.30)	0.34 (0.20)	0.34 (0.43)
Sum of SW	1.20	0.87	
Sum of LW	-1.29	-1.72	
Sum of LW (No Planck)	1.65	1.35	

762
763
764

765 **Table 3:** Summary of correlation coefficients and associated information among key
766 variables. Numbers in bold indicate statistical significance at the 5% level. Symbols
767 are as follows: $\Delta T_G/\Delta T_T$, global/tropical surface temperature change over the 20th
768 century under RCP8.5; $\sigma_{T\ (10yr)}$ SD of decadal global variability in models; ECS,
769 equilibrium climate sensitivity.
770

	ΔT_G	ΔT_T	$\sigma_{T\ (10yr)}$	ECS
ΔT_G	**1**	**0.89**	**0.60**	**0.95**
ΔT_T		**1**	**0.73**	**0.89**
$\sigma_{T\ (10yr)}$			**1**	**0.71**
ECS				**1**

771
772
773

774 **Figures**

775

776 **Figure 1:** Decadal global SD of surface temperature for the CMIP5 models (K), listed
777 in order of increasing SD. Names of models (and the corresponding modelling
778 institutions) are listed in Table S1. Error bars indicate 80% confidence range (Sheskin,
779 2016) from the 200 year pre-industrial experiment sample. Also shown is the
780 observational estimate from Middlemas and Clement (2016).

781

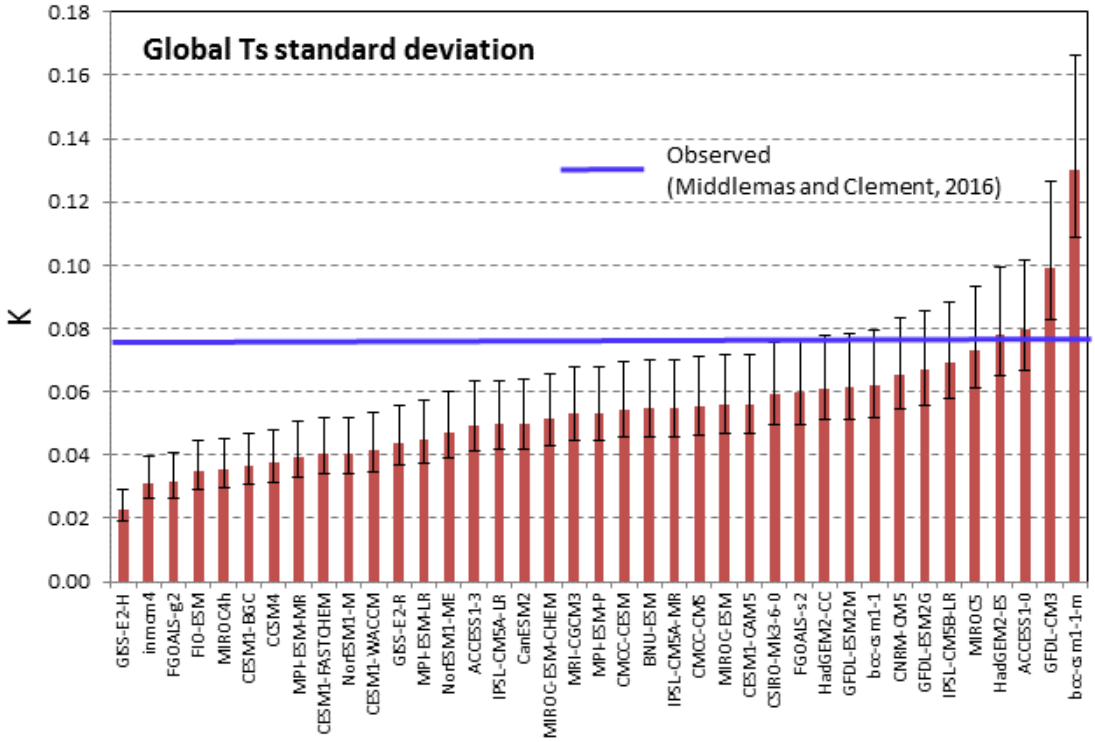

782

Figure 2: (a) Multi-model average of local temperature change (RCP8.5, 2010 to 2100) under RCP8.5 (K); (b) Multi-model average of regression coefficient of the 10-year running mean local temperature against the 10-year running mean tropical mean temperature, multiplied by 1 SD of DCV (unit, K). Calculations are made using 200 years of the pre-industrial experiments (where available). Stippling indicates that in excess of 70% of models agree on the sign of the change (see supplementary material for discussion on choice of stippling threshold).

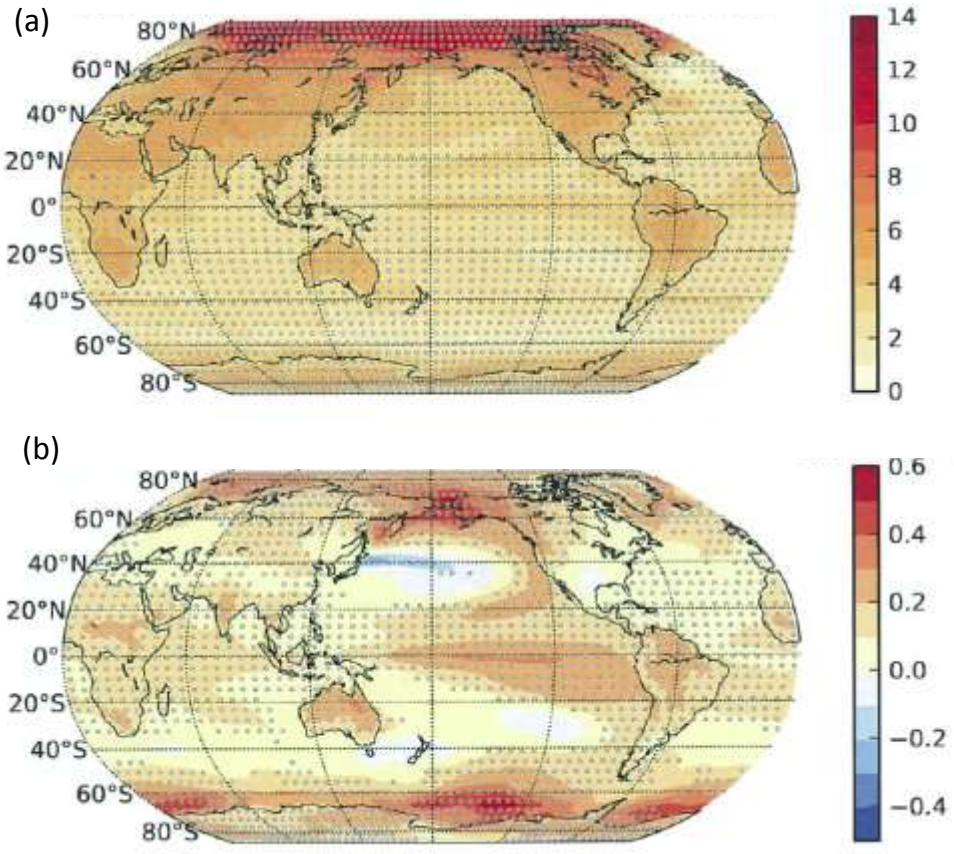

792 **Figure 3:** SD of (a) global, and (b) tropical decadal temperature versus decadal
793 NINO3.4 SDs. Each point represents a CMIP5 model, and the error bars show
794 estimated 80% confidence ranges. Lines of best fit and explained variance are also
795 shown from standard regression.
796

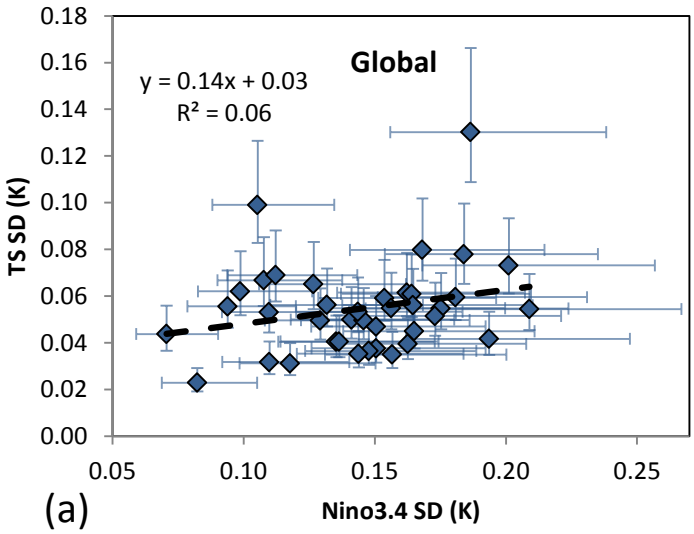

797

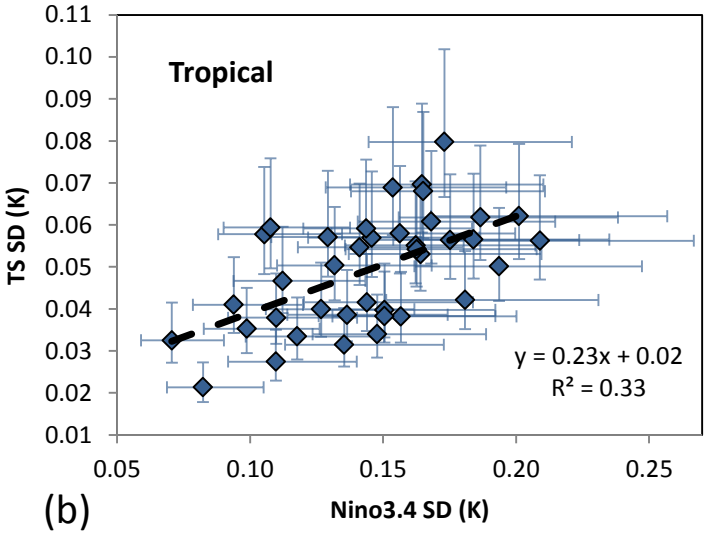

798

799

Figure 4: (a) Total TOA radiative feedback ($W/m^2/K$), versus SD of global temperature (K). (b) Tropical TOA radiative feedback versus tropical temperature SD. Each point represents a CMIP5 model, and x and y error bars show 80% confidence on SD from the PI sampling and feedback from decadal regression respectively. Lines of best fit and explained variance are also shown.

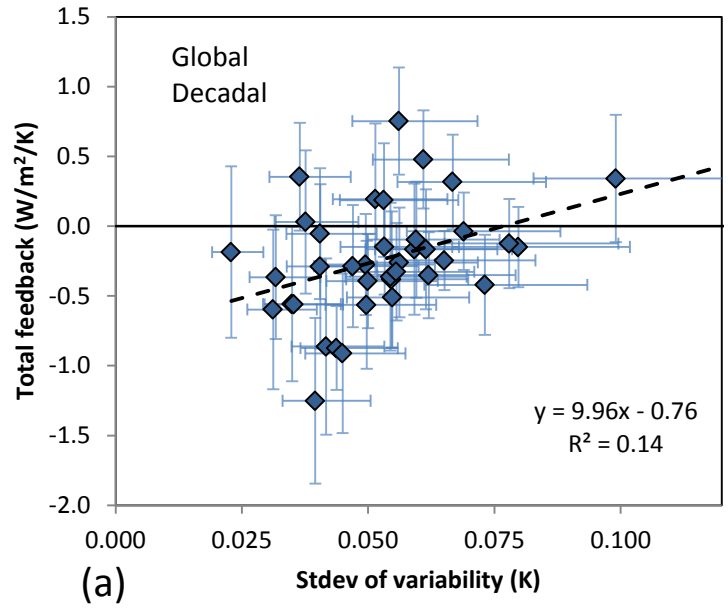

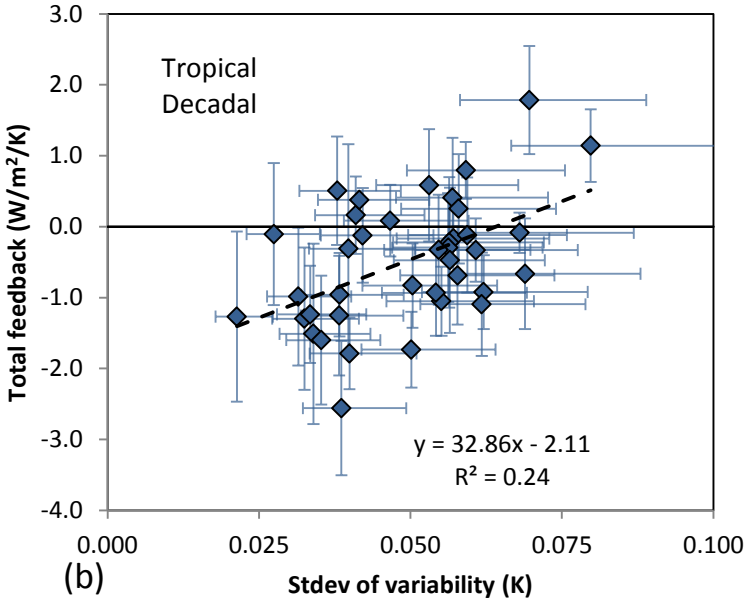

Figure 5: Total tropical (a) LW and (b) SW feedback ($W/m^2/K$), plotted against SD of tropical temperature variability. Each point represents a CMIP5 model, and the error bars show the 80% confidence limit in estimation of the feedback from standard regression. Lines of best fit and explained variance are also shown from standard regression.

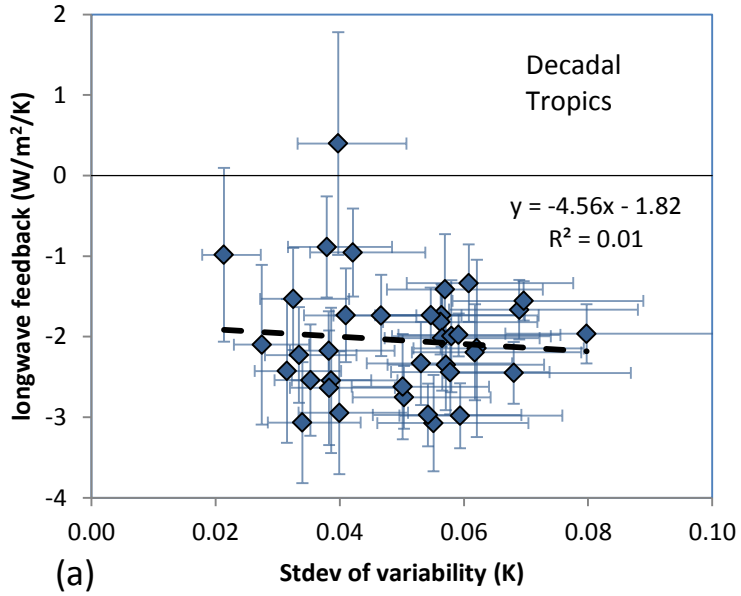

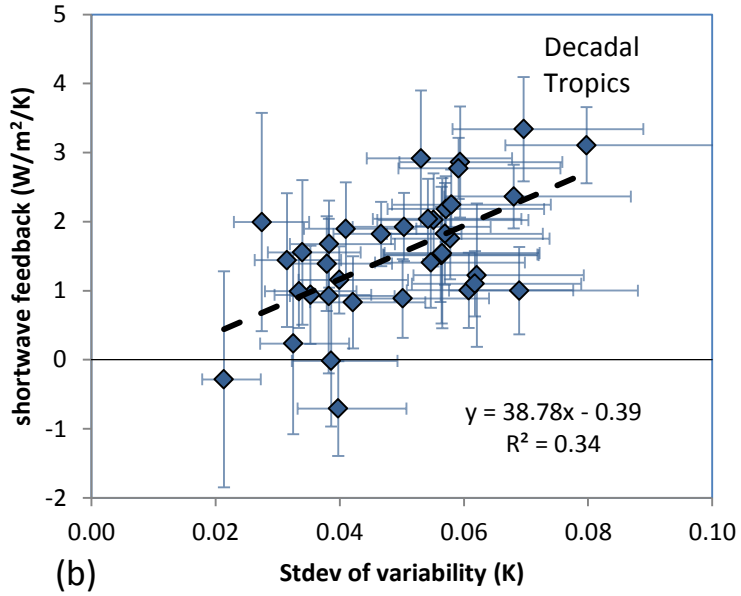

817 **Figure 6:** Net SW feedback, plotted against SW cloud feedback (both *W/m²/K*) for the
818 tropics. Each point represents a CMIP5 model, and the error bars show the 80%
819 confidence limit for standard regression. A line of best fit is also shown, along with
820 explained variance.
821

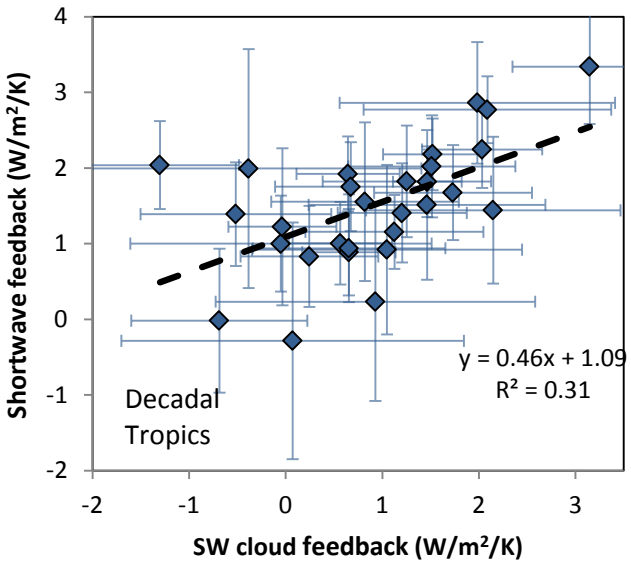

822
823

Figure 7: SW net feedback plotted against LW net feedback (a) globally, and (b) for the tropics only. Each point represents a CMIP5 model, and the error bars show estimated 80% confidence ranges (see Methods for details). Lines of best fit and explained variance are also shown from standard regression.

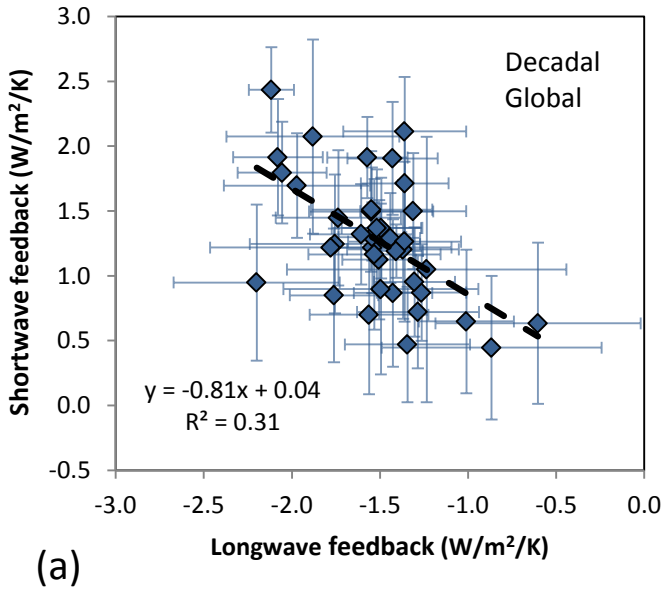

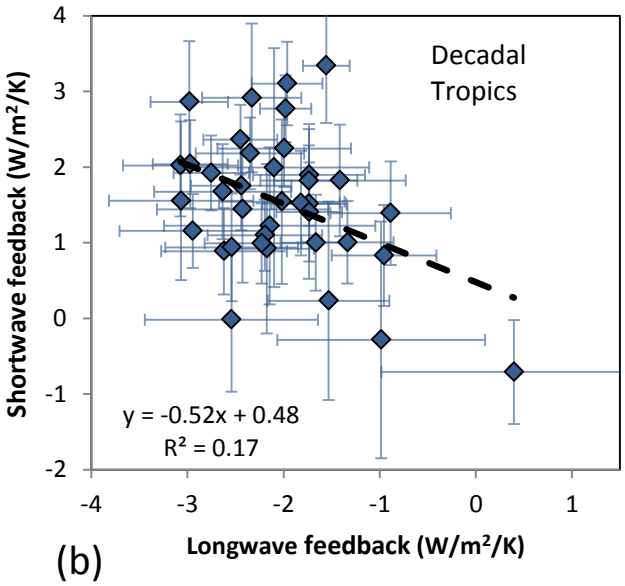

Figure 8: Scatter plots showing: (a) ΔT_G (global temperature change) versus Tropical (30S-30N) temperature decadal SD; (b) Tropical temperature change, versus tropical decadal SD; (c) ΔT_G, TCR versus ECS.

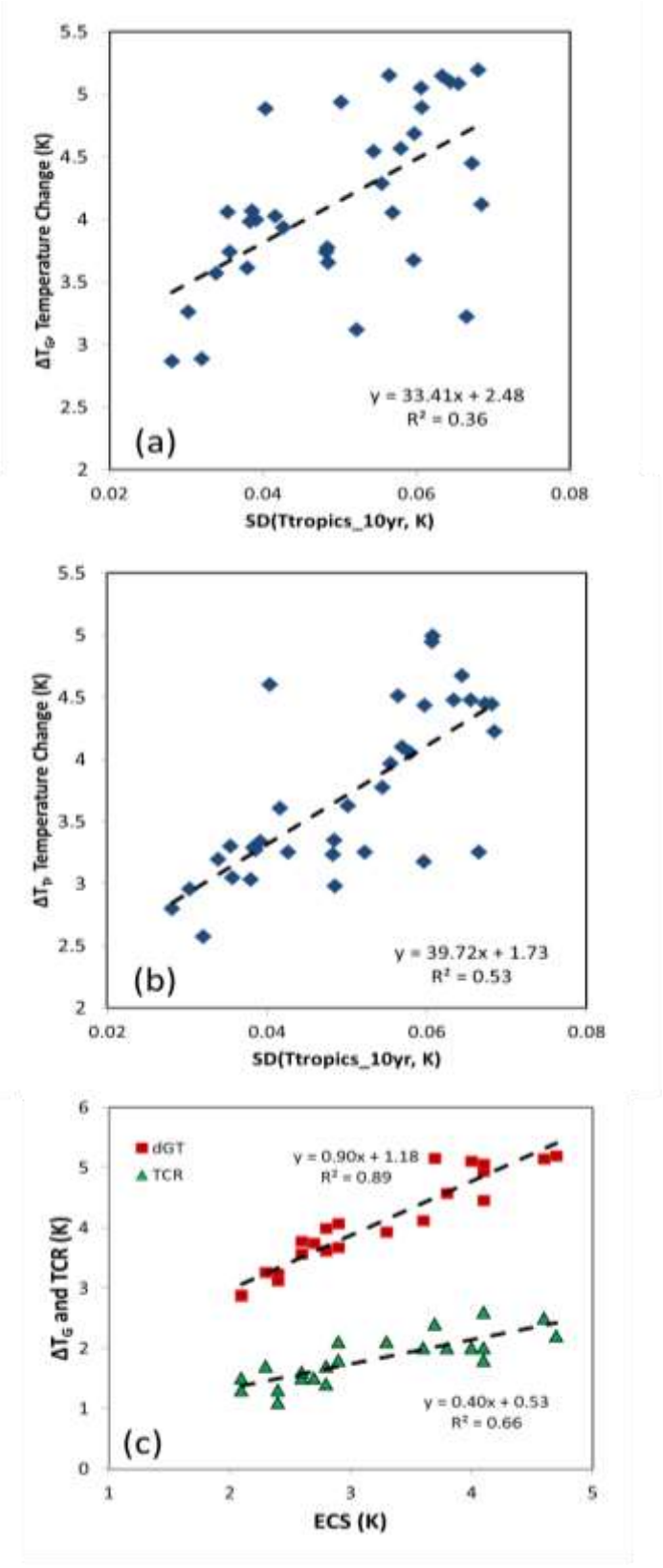

835 **Figure 9:** Scatter plots showing ECS versus tropical SD for (a) CMIP5; (b) CMIP3.
836 Error bars show the 80% confidence range of SD. Also shown are lines of best fit and
837 explained variance from standard regression.

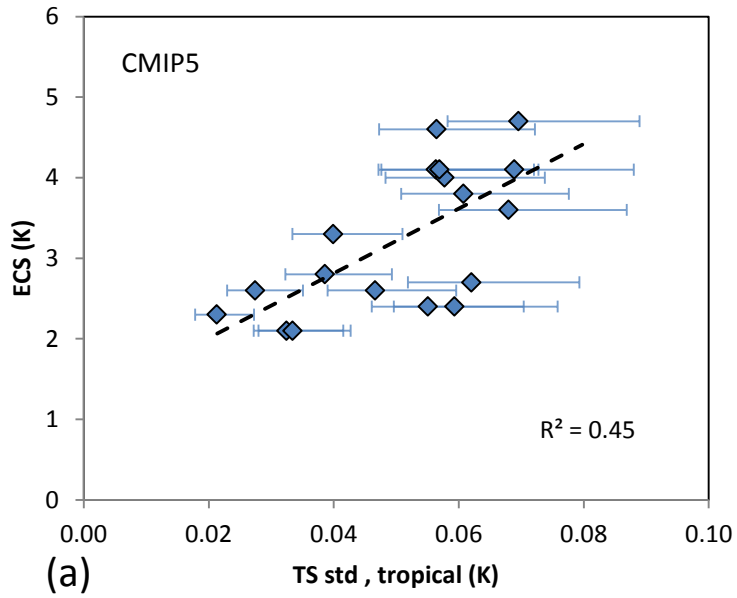

838

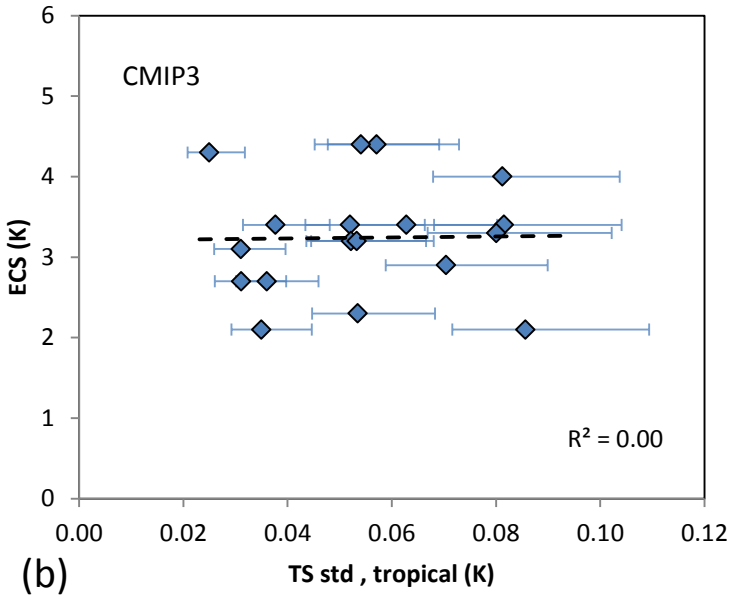

839

Supplementary Material for:

On the role of radiative feedbacks in decadal variability and climate change

Robert Colman and Scott B. Power

Bureau of Meteorology, Melbourne, Victoria, Australia

Contents of this file:

Stippling. Stippling in Figure 2 indicates statistical significance at the 5% level under the assumption that all models are independent (Power et al., 2012). The degree of agreement required to attain this level of statistical significance is based on the Binomial Distribution. The total number of models used, the number of models and the proportion of models (%) agreeing on sign of change indicated by stippling are 21, 15, and $\geq$ 71% respectively.

Temperature reinforcement from decadal feedbacks.

We assume a global temperature change relationship of

$$\Delta T = \frac{H \Delta t}{\rho h C_P}$$

where H is the energy imbalance at the surface, h depth of the mixed layer, ρ the density of sea water, C_P the specific heat of water and Δt the elapsed time (e.g Brown *et al*.,

2014). $H = Q_{TOA} - Q_{BML}$ (bottom mixed layer), and Q_{BML} can be significant on long time scales (Deser *et al*., 2010), but is here assumed to be zero. Mixed layer depth estimates vary, but were calculated as 75m with +/- 1SD of 25m (Baker and Roe, 2009) and by Geoffroy *et al*. (2012) of 77m for the CMIP5 model mean. Assuming H=0.1 W/m^2, (from temperature excursion of 0.05K under a feedback of 2 $W/m^2/K$), h=100m and Δt = 10y results in ΔT=0.075K.

Supplementary material references

Baker, M. B., and G. H. Roe (2009), The shape of things to come: Why is climate change so predictable? J. Clim., 22, 4574–4589

Deser, C., M. A. Alexander, S.-P. Xie, and A. S. Phillips (2010), Sea surface temperature variability: Patterns and mechanisms, Annu. Rev. Mar.Sci., 2, 115–143, doi:10.1146/annurev-marine-120408-151453.

Geoffroy, O., D. Saint-Martin, D. J. L. Olivié, A. Voldoire, G. Bellon, and S. Tytéca (2012), Transient Climate Response in a Two-Layer Energy-Balance Model. Part I: Analytical Solution and Parameter Calibration Using CMIP5 AOGCM Experiments, J. Clim., 26, 1841-1857, doi:10.1175/JCLI-D-12-00195.1.

Power, S.B., F. Delage, R.A. Colman and A.F. Moise (2012): Consensus on 21st century rainfall projections in climate models more widespread than previously thought. Journal of Climate, 25, 3792-3809, doi: 10.1175/JCLI-D-11-00354.1.

887 **Table S1:** The 35 CMIP5 models included in this study: Model name and model host
888 institution. Information summarized from http://cmip-
889 pcmdi.llnl.gov/cmip5/availability.html

Model name(s)	**Model host institution(s)**
ACCESS1.0 ACCESS1.3	Commonwealth Scientific and Industrial Research Organisation (CSIRO) and Bureau of Meteorology
BCC-CSM1-1 BCC-CSM1-1-M	Beijing Climate Center, China Meteorological Administration
BNU-ESM	College of Global Change and Earth System Science, Beijing Normal University
CanESM2	Canadian Centre for Climate Modelling and Analysis
CCSM4	National Center for Atmospheric Research
CESM1-BGC CESM1-CAM5 CESM1-FASTCHEM CESM1-WACCM	National Science Foundation, Department of Energy, National Center for Atmospheric Research
CMCC-CESM CMCC-CM CMCC-CMS	Centro Euro-Mediterraneo per I Cambiamenti Climatici
CNRM-CMS CNRM-CM5	Centre National de Recherches Meteorologiques / Centre Europeen de Recherche et Formation Avancees en Calcul Scientifique
CSIRO-Mk3-6-0	Commonwealth Scientific and Industrial Research Organisation (CSIRO)
FGOALS-g2	LASG, Institute of Atmospheric Physics, Chinese Academy of Sciences; and CESS, Tsinghua University
FGOALS-s2	LASG, Institute of Atmospheric Physics, Chinese Academy of Sciences
FIO-ESM	First Institute of Oceanography
GFDL-CM3 GFDL-ESM2G GFDL-ESM2M	Geophysical Fluid Dynamics Laboratory
GISS-E2-H GISS-E2-R	NASA Goddard Institute for Space Studies
HadGEM2-CC HadGEM2-ES	Met Office Hadley Centre
INM-CM4	Institute of Numerical Mathematics, Russian Academy of Sciences
IPSL-CM5A-LR IPSL-CM5A-MR	Institut Pierre-Simon Laplace

IPSL-CM5B-LR	
MIROC4h MIROC5	Atmosphere and Ocean Research Institute (The University of Tokyo), National Institute for Environmental Studies, and Japan Agency for Marine-Earth Science and Technology
MIROC-ESM MIROC-ESM-CHEM	Japan Agency for Marine-Earth Science and Technology, Atmosphere and Ocean Research Institute (The University of Tokyo), and National Institute for Environmental Studies
MPI-ESM-LR MPI-ESM-MR MPI-ESM-P	Max Planck Institute for Meteorology (MPI-M)
MRI-CGCM3	Meteorological Research Institute
NorESM1-M NorESM1-ME	Norwegian Climate Centre

892 **Table S2:** The 18 CMIP3 models included in this study (see http://www-
893 pcmdi.llnl.gov/ipcc/about_ipcc.php)

bccr_bcm2_0,	Bjerknes Centre for Climate Research
cccma_cgcm3_1 cccma_cgcm3_1_t63	Canadian Centre for Climate Modelling and Analysis
cnrm_cm3	Météo-France / Centre National de Recherches Météorologiques
csiro_mk3_0 csiro_mk3_5	Commonwealth Scientific and Industrial Research Organisation (CSIRO)
gfdl_cm2_0 gfdl_cm2_1	Geophysical Fluid Dynamics Laboratory
giss_aom giss_model_e_h giss_model_e_r	NASA Goddard Institute for Space Studies
iap_fgoals1_0_g	LASG / Institute of Atmospheric Physics
ingv_echam4	Instituto Nazionale di Geofisica e Vulcanologia
inmcm3_0	Institute for Numerical Mathematics
ipsl_cm4	Institut Pierre-Simon Laplace
miroc3_2_hires miroc3_2_medres	Center for Climate System Research (The University of Tokyo), National Institute for Environmental Studies, and Frontier Research Center for Global Change (JAMSTEC)
miub_echo_g	Meteorological Institute of the University of Bonn, Meteorological Research Institute of KMA, and Model and Data group
mpi_echam5	Max Planck Institute for Meteorology
mri_cgcm2_3_2a	Meteorological Research Institute

ncar_ccsm3_0 ncar_pcm1	National Center for Atmospheric Research
ukmo_hadcm3 ukmo_hadgem1	Met Office Hadley Centre

894

895

Figure S1: Example of (a) LW, (b) SW and (c) total global mean TOA radiation as a function of decadal global mean temperature for model ACCESS1.0. Individual months (blue diamonds) and annual means (black diamonds) are shown. Linear regression equations and explained variance on the annual means are also shown from standard regression. In (c), the red line shows the expected relationship if only Planck cooling were to operate.